Shape coexistence and β decay of ^{70}Br within a beyond-mean-field approach

A. Petrovici*

Horia Hulubei National Institute for Physics and Nuclear Engineering, R-077125 Bucharest, Romania

(Received 30 May 2017; revised manuscript received 4 October 2017; published 12 February 2018)

β-decay properties of the odd-odd $N = Z$ ^{70}Br nucleus are self-consistently explored within the beyond-mean-field complex excited VAMPIR variational model using an effective interaction obtained from a nuclear matter G-matrix based on the charge-dependent Bonn CD potential and an adequate model space. Results on superallowed Fermi β decay of the ground state and Gamow-Teller decay of the 9^+ isomer in ^{70}Br correlated with the shape coexistence and mixing effects on the structure and electromagnetic properties of the populated states in the daughter nucleus ^{70}Se are presented and compared with available data.

DOI: 10.1103/PhysRevC.97.024313

I. INTRODUCTION

The $A \approx 70$ proton-rich nuclei relevant for the astrophysical rp process represent a testing ground for the beyond-mean-field models aiming to realistically describe their exotic structure and dynamics induced by shape coexistence and mixing. Close to the $N = Z$ line the structure of these nuclei is influenced by the competition between like-nucleon and neutron-proton pairing correlations in the $T = 1$ and $T = 0$ channels and the isospin-symmetry-breaking interactions as it is revealed in previous investigations by the present author and a coworker [1–3]. A difficult task for the theoretical models is the simultaneous description of the structure and β-decay properties including the superallowed Fermi and the Gamow-Teller (GT) strength distributions. In particular, in the $A = 70$ isovector triplet, besides the understanding of the isospin-related phenomena and of the competing decays of the ground state of the $Z = N + 2$ ^{70}Kr [1,2], the description of the β-decay properties of the ground state and the 9^+ isomer in ^{70}Br represent a new challenge for theory. Various coexistence phenomena displayed by the structure and dynamics of proton-rich nuclei in the $A \approx 70$ mass region have been extensively investigated within the complex excited VAMPIR model [1–7] and the results indicate good agreement with the available data. Robust predictions on weak interaction rates in the x-ray burst environment have been presented based on the experimentally confirmed results on decay properties under terrestrial conditions [2,7]. The present study is the first attempt at a comprehensive self-consistent understanding of shape coexistence effects on the decay of the ground state and 9^+ isomeric state in ^{70}Br correlated with the structure and electromagnetic properties of the populated states in the ^{70}Se daughter nucleus in the frame of the complex excited VAMPIR model. The predictions could be tested by the data from a recent experiment at Riken published after the first submission of my paper [8].

In the next section will be presented the variational procedure underlying the complex excited VAMPIR model and the main ingredients of the theory. In Sec. III I will discuss results on shape coexistence effects on superallowed Fermi and Gamow-Teller β decay of ^{70}Br, and the structure and electromagnetic properties of the daughter states in ^{70}Se. Some concluding remarks are presented in Sec. IV.

II. THEORETICAL FRAMEWORK

The basic building blocks of the complex excited VAMPIR model are Hartree-Fock-Bogoliubov (HFB) vacua. The corresponding HFB transformations are essentially complex allowing for proton-neutron, parity, and angular momentum mixing being restricted by time-reversal and axial symmetry. The use of essentially complex unitary transformations creates the possibility to account for natural- and unnatural-parity two-body correlations, as well as neutron-proton pairing correlations in both $T = 1$ and $T = 0$ channels. The restoration of broken symmetries (nucleon numbers, parity, total angular momentum) is done before variation using projection techniques. The symmetry-projected configurations are used as trial wave functions in chains of successive variational calculations for each considered symmetry. Within the variational procedure are determined the underlying HFB transformations and the configuration mixing ([1] and references therein). The complex excited VAMPIR model, allowing the use of large model spaces and realistic effective interactions, goes far beyond the abilities of the conventional shell-model configuration-mixing approach, making possible large-scale nuclear structure studies.

In the present work I extended the previous investigations on the structure of even-spin positive-parity states in the $A = 70$ isovector triplet in the frame of the complex excited VAMPIR model. I used the same model space and effective interaction involved in our studies on isospin-related phenomena including superallowed Fermi β-decay, as well as Gamow-Teller decay properties [1–3]. For the investigation of $A \approx 70$ nuclei a ^{40}Ca core is used and the model space is built out of the $1p_{1/2}, 1p_{3/2}, 0f_{5/2}, 0f_{7/2}, 1d_{5/2}$, and $0g_{9/2}$ oscillator orbits for

*spetro@nipne.ro

the valence protons and neutrons. One starts with an isospin symmetric basis and then for the proton single-particle levels Coulomb shifts are introduced induced by the ^{40}Ca core obtained by spherically symmetric Hartree-Fock calculations involving the Gogny-interaction D1S in a 21 major-shell basis [1]. The effective two-body interaction is constructed from a nuclear matter G matrix based on the charge-dependent Bonn CD potential. The G matrix is renormalized by adding short-range (0.707 fm) Gaussians in the $T = 1$ and $T = 0$ channels enhancing the pairing correlations. To influence the onset of deformation and the oblate-prolate competition in the structure of the investigated nuclei, monopole shifts of -500 keV have been introduced for the matrix elements of the form $\langle 1p1d_{5/2}; IT = 0|\hat{G}|1p1d_{5/2}; IT = 0\rangle$, where $1p$ denotes either the $1p_{1/2}$ or the $1p_{3/2}$ orbit, and of -370 keV for $\langle 0g_{9/2}0f; IT = 0|\hat{G}|0g_{9/2}0f; IT = 0\rangle$, where $0f$ denotes either the $0f_{5/2}$ or the $0f_{7/2}$ orbitals [1]. The shifts for the latter matrix elements have been varied from -250 keV to -400 keV within the investigations of the properties of $A \approx 70$ nuclei. The Hamiltonian includes the two-body matrix elements of the Coulomb interaction of the valence protons.

III. RESULTS AND DISCUSSION

For the investigation of the structure of the lowest few states of spin 0^+, 2^+, 4^+, 6^+, 8^+, and 10^+ in ^{70}Se 22 orthogonal many-nucleon excited VAMPIR (EXVAM) configurations have been constructed. The mixing of the differently deformed projected configurations in the intrinsic system in the structure of the wave functions is obtained diagonalizing the residual interaction between the states building the many-body basis specific for each considered symmetry.

In ^{70}Se the evolution of shape mixing with increasing spin and excitation energy is indicated by the structure of the wave functions for the investigated states. Particular effects of shape coexistence and mixing are reflected by the electromagnetic properties. The structure of the wave functions for the lowest two states of spin 0^+, 2^+, 4^+, and 6^+ indicates 48%, 58%, 54%, and 81% prolate content for the yrast states, respectively, while for the first excited states the oblate content is dominant, except for spin 0^+, amounting to 43%, 59%, 55%, and 81%, respectively. For the calculated lowest five states of spin 8^+ and 10^+ the prolate-oblate mixing is presented in Table I indicating the contribution of the EXVAM configurations bringing at least 2% to the total amplitude. With increasing spin the states dominated by oblate components go higher in excitation energy, the third 8^+ and the fifth 10^+ building the $o(p)$ band manifesting strong oblate content. The effect of the prolate-oblate mixing is reflected by the spectroscopic quadrupole moments presented in Table II for the lowest few states of a given spin labeled according to increasing excitation energy. Small variations inside the range indicated above for the monopole shifts could induce changes in the shape mixing and consequently in the spectroscopic quadrupole moments, but more precise experimental values than the available ones [9] are required to improve the effective interaction. Based on the available experimental information in the region effective charges of $e_p = 1.2$ and $e_n = 0.2$ have been used.

TABLE I. The amount of mixing for the lowest 8^+ and 10^+ states in ^{70}Se. The contributions (of at least 2%) of EXVAM configurations are indicated in decreasing order.

I[$\hbar$]	prolate content	oblate content
8^+_1	84(3)(2)(2)%	2%
8^+_2	47(11)(7)(4)(4)(3)(2)%	18%
8^+_3	12(5)(2)(2)%	73%
8^+_4	59(12)(6)(5)(4)(3)(2)(2)%	4%
8^+_5	56(11)(8)(6)(5)(5)(4)(2)%	
10^+_1	51(39)(2)(2)%	
10^+_2	40(40)(7)(5)(2)(2)(2)%	
10^+_3	54(20)(10)(5)(2)(2)%	
10^+_4	48(12)(10)(5)(5)%	13%
10^+_5	10(2)%	84%

Figure 1 illustrates the EXVAM spectrum constructed based on the $B(E2)$ values connecting the states compared with experimental data [10–12], including the new results [8] published after the first submission of the paper. The bands are labeled according to the deformation in the intrinsic system of the dominant configurations in the structure of the corresponding states. The decay pattern of the second and third 8^+ states in the theoretical spectrum compare rather well with the new excited states and low-intensity γ-ray transitions reported in Ref. [8]. The theoretical candidate for the new experimental 8^+ state is the third 8^+ belonging the the $o(p)$ band dominated by oblate deformed configurations. The second 8^+ state dominated by prolate components, similar to the experimental data, is feeding the second and the third 6^+ states, but very weakly the yrast 6^+ and 8^+ states. The existing deficiencies in the theoretical spectrum could be influenced by small changes in the monopole shifts as well as by the higher-lying configurations not included in the presently involved EXVAM many-nucleon bases. More experimental data are needed to improve the theoretical results on shape coexistence and mixing including the existence of the first excited 0^+ state predicted to be almost degenerate with the first excited 2^+ state.

The calculated $B(E2)$ values are presented in Table III. The latest measurements give for the $B(E2)$ strengths the values 342(19), 370(24), 530(96) $e^2\,fm^4$ for the decay of the yrast 2^+,

TABLE II. Spectroscopic quadrupole moments (in $e\,fm^2$) for the lowest EXVAM states of ^{70}Se.

I[$\hbar$]		I[$\hbar$]	
2^+_1	−6.8	8^+_1	−65.6
2^+_2	4.1	8^+_2	−42.1
4^+_1	−7.2	8^+_3	28.2
4^+_2	0.1	8^+_4	−61.4
6^+_1	−42.5	8^+_5	−62.0
6^+_2	33.0	10^+_1	−64.0
6^+_3	−59.2	10^+_2	−70.9
6^+_4	−56.9	10^+_3	−66.0
6^+_5	−32.4	10^+_4	−48.2
		10^+_5	41.2

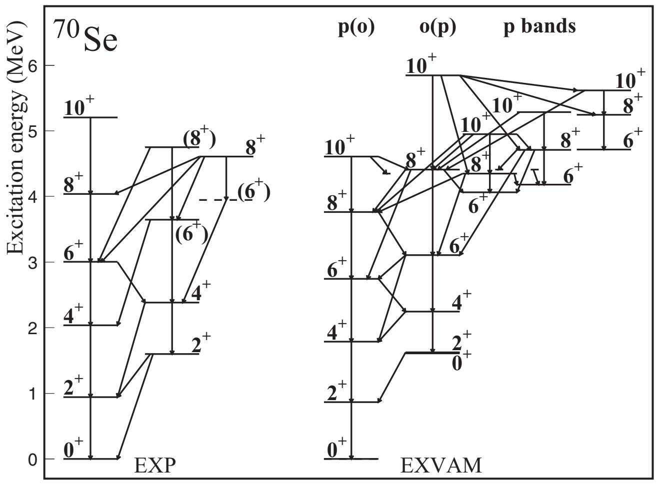

FIG. 1. The complex excited VAMPIR spectrum for ^{70}Se compared with experimental data [8,10–12] (the arrows indicate $E2$ transitions).

4^+, and 6^+ states, respectively [9]. The complex excited VAMPIR results reproduce the experimental trend, while the maximum deviation of 79% with respect to data is for spin 4^+. The EXVAM model indicates better agreement with the measured $B(E2)$ values than the generator coordinate calculations with Gaussian overlap approximation using Gogny D1S interaction [9]. Published together with the new experimental results the shell-model calculations using a $p_{1/2}$, $p_{3/2}$, $f_{5/2}$, $g_{9/2}$ model space and two different interactions indicate smaller deviations from the $B(E2)$ data only up to spin 6^+, but for the interaction giving less accuracy for the excitation energies [8].

The fragmentation of the $B(E2)$ strength decaying a given state, as well as the significant transition strengths connecting states of the same spin represent fingerprints of shape mixing. For the transitions connecting the lowest two states of spin 2^+, 4^+, 6^+, and 8^+ the calculated $B(E2)$ values are 636, 617, 385, 27 $e^2 fm^4$, respectively, while maximum value for 8^+ states $B(E2; 8_3 \rightarrow 8_2)$ amounts to 288 $e^2 fm^4$. Very strong $M1$ transitions connect 10^+ states in Fig. 1: $B(M1; 10_2 \rightarrow 10_1) = 1.526\ \mu_N^2$ and $B(M1; 10_3 \rightarrow 10_1) = 1.319\ \mu_N^2$. The strongest $M1$ branches for the 8^+ states depicted in Fig. 1 amount to $B(M1; 8_4 \rightarrow 8_1) = 0.522\ \mu_N^2$ and $B(M1; 8_4 \rightarrow 8_2) = 0.460\ \mu_N^2$. For the lower spin states significant $B(M1)$ values have been obtained only for the 6^+ states: $B(M1; 6_4 \rightarrow 6_3) = 0.391\ \mu_N^2$ and $B(M1; 6_5 \rightarrow 6_3) = 0.513\ \mu_N^2$. The results have been obtained using free nucleon values for the gyromagnetic factors. Within the same theoretical framework I investigated the superallowed Fermi β decay of the ground state and the Gamow-Teller decay of the 9^+ isomer in ^{70}Br. The structure of the ground state built using a 22-dimensional EXVAM basis indicates 70% prolate content [1]. For the description of the 9^+ state 30 EXVAM configurations have been constructed and the wave function for this state is built out of prolate configurations, the two main ones making 96% of the total amplitude. The calculated spectroscopic quadrupole moment for the 9^+ isomer is $-64.2\ efm^2$. For the daughter 8^+ and 10^+ states in ^{70}Se up to 70 EXVAM configurations have been calculated.

TABLE III. $B(E2; I \rightarrow I-2)$ values (in $e^2 fm^4$) for the bands presented in Fig. 1. The strengths for secondary branches (from the leftmost to the rightmost bands) are given in parentheses. The strengths given in brackets are not shown in the figure.

I[$\hbar$]	$p(o)$	$o(p)$	p bands
2^+	473	476	
4^+	706	733	
6^+	738(92)	730(58)	
8^+	781(78)	404(109)(49)(154)	
10^+	564(86)(55)	477(109)(53)(147)	
8_2^+			284(276)(179)
10_2^+			515(271)(40)(46)
8_4^+			357(23)(329)
10_3^+			613(90)
8_5^+			305[132][187]
10_4^+			556(106)

The Fermi and Gamow-Teller reduced transition probabilities treated on the same footing are written as

$$B_{if}(F) = \frac{1}{2J_i + 1}|M_F|^2, \tag{1}$$

$$B_{if}(GT) = \frac{1}{2J_i + 1}\left(\frac{g_A}{g_V}\right)^2 |M_{GT}|^2, \tag{2}$$

where $g_A/g_V = -1.26$. Previous investigations by the present author and a coworker concerning the effects of missing spin-orbit partners in the model space on the Gamow-Teller decay of the ^{72}Kr nucleus [7] revealed very small changes for the strength distributions, accumulated strengths, and half-lives obtained in an extended model space. We compared the strength distributions for the decay of the lowest two 0^+ and 2^+ states in ^{72}Kr obtained in the presently used model space and a very large one including the spin-orbit partners. A missing Gamow-Teller strength of $\approx$10% attributed to the Δ excitation [13] is not included in the present results. The Fermi and Gamow-Teller nuclear matrix elements between the initial ($|\xi_i J_i>$) and the final ($|\xi_f J_f>$) states of spin J_i and J_f,

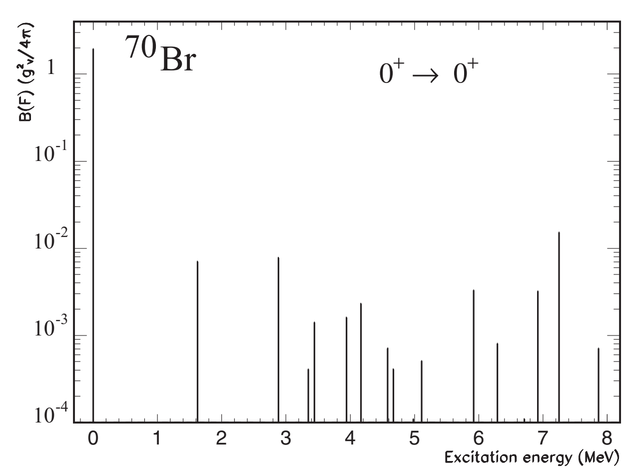

FIG. 2. The Fermi strength distribution for the decay of the ground state of ^{70}Br to ^{70}Se obtained within complex excited VAMPIR model.

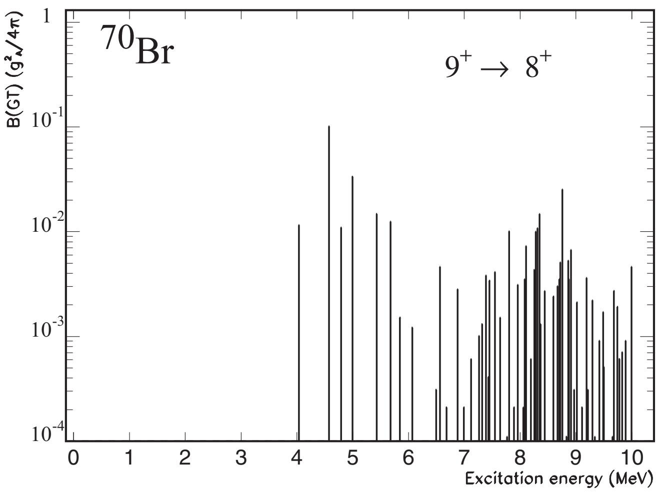

FIG. 3. The Gamow-Teller strength distribution for the decay of the 9^+ isomer in ^{70}Br to 8^+ states in ^{70}Se obtained within complex excited VAMPIR model.

respectively,

$$M_F \equiv (\xi_f J_f||\hat{1}||\xi_i J_i) = \delta_{J_i J_f} \sum_{ab} M_F(ab)(\xi_f J_f||[c_a^\dagger \tilde{c}_b]_0||\xi_i J_i), \quad (3)$$

$$M_{GT} \equiv (\xi_f J_f||\hat{\sigma}||\xi_i J_i) = \sum_{ab} M_{GT}(ab)(\xi_f J_f||[c_a^\dagger \tilde{c}_b]_1||\xi_i J_i), \quad (4)$$

are composed of the reduced single-particle matrix elements of the unit operator $\hat{1}$, $M_F(ab) = (a||\hat{1}||b)$, and Pauli spin operator $\hat{\sigma}$, $M_{GT} = 1/\sqrt{3}(a||\hat{\sigma}||b)$, and the reduced one-body transition densities calculated using the harmonic oscillator wave functions. For β^+ decay and electron capture $c_a^\dagger$ is the neutron creation operator and $\tilde{c}_b$ is the proton annihilation operator and the sum runs over the valence nucleons.

In Fig. 2 is presented the Fermi strength distribution for the decay of the ground state of ^{70}Br to 0^+ states in ^{70}Se. The results

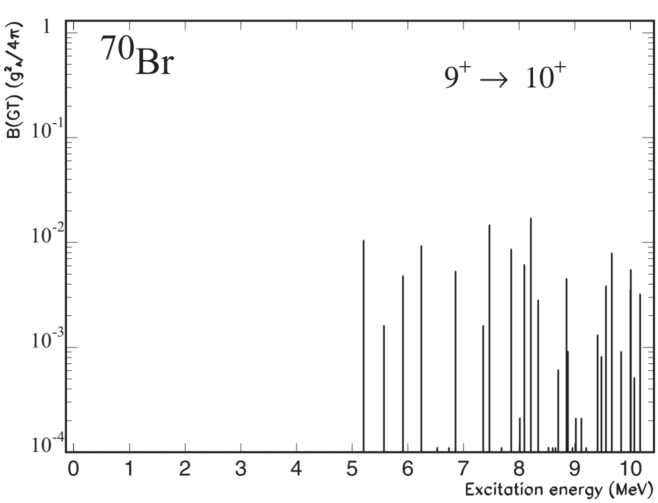

FIG. 4. The same as in Fig. 3, but for 10^+ states in ^{70}Se.

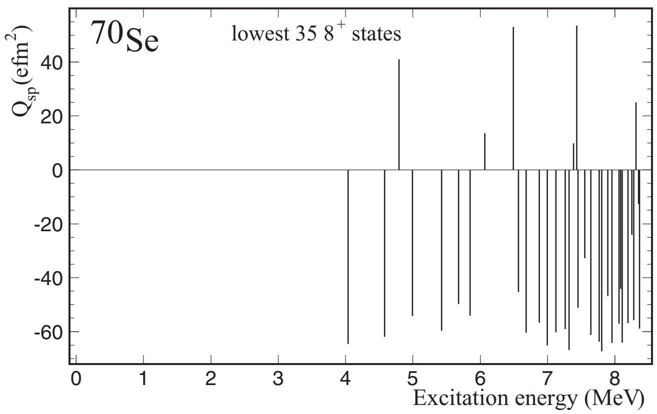

FIG. 5. Spectroscopic quadrupole moments of 8^+ Gamow-Teller daughter states in ^{70}Se.

indicate that the depletion of the ground-to-ground transition has an upper limit of 2% and the missing strength is distributed over many 0^+ states. Part of these states could finally feed the yrast 2^+ state in ^{70}Se, but a test of these predictions requires experimental results obtained using a total absorption spectrometer. It is worthwhile to mention that it is difficult to disentangle between the effects of the isospin nonconserving forces and shape mixing on the missing strength in the ground-to-ground decay at least based on the presently available data.

In Figs. 3 and 4 are depicted the Gamow-Teller strength distributions for the decay of the 9^+ isomer in ^{70}Br to 8^+ and 10^+ states in ^{70}Se, respectively. The excitation energy of the yrast 8^+ and 10^+ states is slightly changed to the experimental value (the shifts amount to 300 keV and 500 keV for the 8^+ and 10^+ states, respectively), while for the excited states the relative values with respect to the yrast ones are considered. It is worthwhile to mention that the results could be slightly changed even at lower energies by higher configurations, which are not included in the present calculations. Very weak transition strengths have been found for the decay of the 9^+ isomer to 9^+ states in ^{70}Se. The analysis of the structure of the lowest five significant Gamow-Teller branches, the strongest being the one feeding the 8_2^+ state, indicates that maximum contribution is coming from $g_{9/2}^{\nu} g_{9/2}^{\pi}$ matrix elements. For the GT branch feeding the fourth 8^+ state almost equal contributions

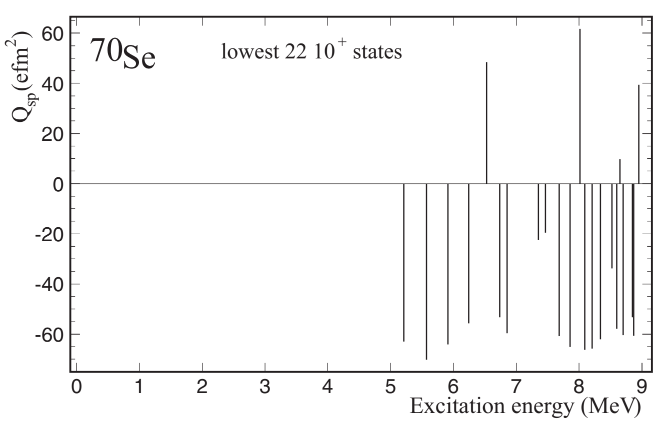

FIG. 6. The same as in Fig. 5, but for 10^+ states in ^{70}Se.

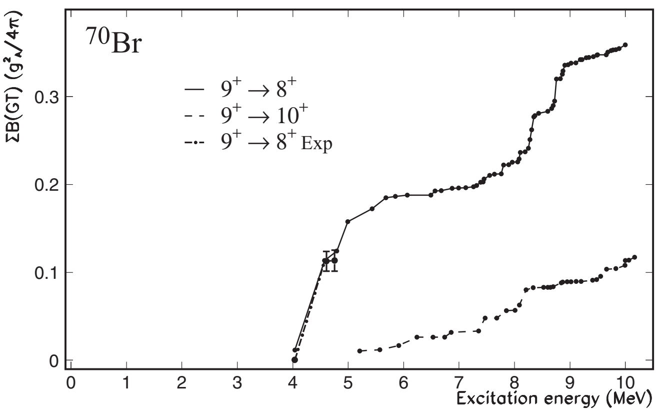

FIG. 7. The complex excited VAMPIR Gamow-Teller accumulated strength for the decay of the 9^+ isomer in ^{70}Br to 8^+ and 10^+ states in ^{70}Se compared to the data for 8^+ states [8,12].

are brought by the $p^{\nu}_{1/2}p^{\pi}_{3/2}$, $p^{\nu}_{3/2}p^{\pi}_{3/2}$, and $g^{\nu}_{9/2}g^{\pi}_{9/2}$ matrix elements. Coherent contributions are produced by the $p^{\nu(\pi)}_{1/2}p^{\pi(\nu)}_{3/2}$, $p^{\nu}_{3/2}p^{\pi}_{3/2}$, $f^{\nu}_{5/2}f^{\pi}_{5/2}$, $d^{\nu}_{5/2}d^{\pi}_{5/2}$ matrix elements, but the weaker GT branches show cancellation of all these contributing matrix elements. The strength distribution depicted in Fig. 3 for the lowest daughter states is nicely confirmed by the recently published experimental results presenting upper limits for the observed states [8]. In Fig. 5 are depicted the spectroscopic quadrupole moments of the lowest 35 8^+ Gamow-Teller daughter states in ^{70}Se illustrating the evolution of shape coexistence and mixing with increasing excitation energy. The structure of the wave functions for the states displaying small spectroscopic quadrupole moments indicates strong oblate-prolate mixing. It is worthwhile to mention that significant strength manifests the GT branch feeding the third 8^+ state dominated by an oblate component (84%) corresponding to the newly populated 8^+ state reported in Ref. [8]. A similar evolution of shape coexistence and mixing with increasing excitation energy is manifested in the structure of the 10^+ GT daughter states in ^{70}Se as it can be inferred from Fig. 6. As for the 8^+ states strong oblate-prolate mixing is manifested by the structure of the 10^+ states characterized by small spectroscopic quadrupole moments.

The Gamow-Teller accumulated strengths for the decay of the 9^+ isomer to 8^+ and 10^+ states depicted in Fig. 7 indicate agreement with the data for 8^+ states [8,12]. The half-life for the Gamow-Teller decay of the 9^+ isomer is given by

$$\frac{1}{T_{1/2}} = \frac{1}{K}\sum_{E_f} f(Z,E_f)B_{if}(GT), \tag{5}$$

where E_f denotes the energy of the final state, $K = 6146$ s and the Fermi integrals $f(Z,E_f)$ are taken from Ref. [14]. The complex excited VAMPIR half-life for the 9^+ isomer using beta window $Q_{EC} = 12.19$ MeV [15], not including a ≈10% missing strength attributed to Δ excitation [13], amounts to 2.3 s indicating agreement with the experimental values of 2.19(9) s [16] and 2.157(50) s [8].

IV. CONCLUSIONS

This paper presents the first comprehensive results on the superallowed Fermi β decay of the ground state and the Gamow-Teller decay of the 9^+ isomer in ^{70}Br and the structure and electromagnetic properties of the states populated in ^{70}Se daughter nucleus in the frame of the complex excited VAMPIR model. New aspects of shape coexistence are revealed within the same theoretical framework, involving the same effective interaction and model space, previously used to investigate isospin-related phenomena in the $A = 70$ isovector triplet. The agreement with the available data, including the new ones published after the first submission for publication of the present results on the investigated properties of the 9^+ isomer in ^{70}Br gives support to the excited VAMPIR scenario on the effects of shape coexistence in these proton-rich nuclei. To improve the estimation of the shape coexistence effects on the electromagnetic properties in ^{70}Se one could refine the effective interaction and increase the dimension of the many-nucleon excited VAMPIR bases. Small changes in the monopole shifts could induce changes in the shape mixing and consequently in the spectroscopic quadrupole moments. Precise data on the spectroscopic quadrupole moments of the lowest two 2^+ states in ^{70}Se expected in the near future from Coulomb excitation experiments at CERN-ISOLDE may help to refine the effective interaction. Changes in the effective interaction as well as additional correlations from higher-lying configurations not included in the presently involved EXVAM bases specific for each spin could influence the spectrum, the Gamow-Teller strength distributions, and the Fermi branches at low energies. Of course, precise data obtained using a total absorption spectrometer could help to refine the theoretical results.

ACKNOWLEDGMENTS

This work has been supported by the Ministry of Research and Innovation (Romania), project CERN-RO-EXONTEX, Contract No. 03/2016 and Program NUCLEU.

[1] A. Petrovici, Phys. Rev. C **91**, 014302 (2015).
[2] A. Petrovici and O. Andrei, Phys. Rev. C **92**, 064305 (2015).
[3] A. Petrovici, Phys. Scr. **92**, 064003 (2017).
[4] A. Petrovici, K. W. Schmid, O. Radu, and A. Faessler, Phys. Rev. C **78**, 044315 (2008).
[5] A. Petrovici, K. W. Schmid, O. Andrei, and A. Faessler, Phys. Rev. C **80**, 044319 (2009).
[6] A. Petrovici, K. W. Schmid, and A. Faessler, Progr. Part. Nucl. Phys. **66**, 287 (2011).
[7] A. Petrovici and O. Andrei, Eur. Phys. J. A **51**, 133 (2015).
[8] A. I. Morales *et al.*, Phys. Rev. C **95**, 064327 (2017).
[9] J. Ljungvall, A. Gorgen, M. Girod, J. P. Delaroche, A. Dewald, C. Dossat, E. Farnea, W. Korten, B. Melon, R. Menegazzo, A. Obertelli, R. Orlandi, P. Petkov, T. Pissulla, S. Siem, R. P. Singh, J. Srebrny, C. Theisen, C. A. Ur, J. J. Valiente-Dobon, K. O. Zell, and M. Zielinska, Phys. Rev. Lett. **100**, 102502 (2008).
[10] T. Mylaeus, J. Phys. G: Nucl. Part. Phys. **15**, L135 (1989).

[11] A. Piechaczek, E. F. Zganjar, J. C. Batchelder, B. D. Macdonald, W. D. Kulp, S. D. Paul, R. Terry, and J. L. Wood, Phys. Rev. C **62**, 054317 (2000).
[12] G. Gürdal and E. A. McCutchan, Nucl. Data Sheets **136**, 1 (2016).
[13] M. Ichimura, H. Sakai, and T. Wakasa, Progr. Part. Nucl. Phys. **56**, 446 (2006).
[14] N. B. Gove and M. J. Martin, Nucl. Data Tables **10**, 205 (1971).
[15] M. Karny, L. Batist, D. Jenkins, M. Kavatsyuk, O. Kavatsyuk, R. Kirchner, A. Korgul, E. Roeckl, and J. Zylicz, Phys. Rev. C **70**, 014310 (2004).
[16] B. Vosicki *et al.*, Nucl. Instrum. Methods Phys. Res. **186**, 307 (1981).